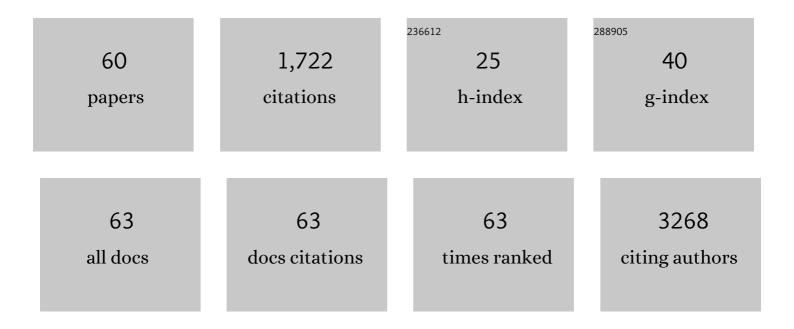
## Siver Andreas Moestue

List of Publications by Year in descending order

Source: https://exaly.com/author-pdf/3324827/publications.pdf Version: 2024-02-01



#	Article	IF	CITATIONS
1	Detection of colorectal polyps in humans using an intravenously administered fluorescent peptide targeted against c-Met. Nature Medicine, 2015, 21, 955-961.	15.2	231
2	Distinct choline metabolic profiles are associated with differences in gene expression for basal-like and luminal-like breast cancer xenograft models. BMC Cancer, 2010, 10, 433.	1.1	93
3	HR MAS MR Spectroscopy in Metabolic Characterization of Cancer. Current Topics in Medicinal Chemistry, 2011, 11, 2-26.	1.0	86
4	Cancer cachexia associates with a systemic autophagy-inducing activity mimicked by cancer cell-derived IL-6 trans-signaling. Scientific Reports, 2017, 7, 2046.	1.6	85
5	Microemulsion electrokinetic chromatography in suppressed electroosmotic flow environment. Journal of Chromatography A, 2000, 876, 201-211.	1.8	81
6	MRS and MRSI guidance in molecular medicine: targeting and monitoring of choline and glucose metabolism in cancer. NMR in Biomedicine, 2011, 24, 673-690.	1.6	81
7	Inhibition of O-GlcNAc transferase activity reprograms prostate cancer cell metabolism. Oncotarget, 2016, 7, 12464-12476.	0.8	71
8	Metabolic reprogramming supports the invasive phenotype in malignant melanoma. Cancer Letters, 2015, 366, 71-83.	3.2	70
9	18F-Fluciclovine PET/MRI for preoperative lymph node staging in high-risk prostate cancer patients. European Radiology, 2018, 28, 3151-3159.	2.3	59
10	Interplay of choline metabolites and genes in patient-derived breast cancer xenografts. Breast Cancer Research, 2014, 16, R5.	2.2	45
11	Estrogen Receptor α Promotes Breast Cancer by Reprogramming Choline Metabolism. Cancer Research, 2016, 76, 5634-5646.	0.4	45
12	Metabolic biomarkers for response to PI3K inhibition in basal-like breast cancer. Breast Cancer Research, 2013, 15, R16.	2.2	42
13	Glutamine to proline conversion is associated with response to glutaminase inhibition in breast cancer. Breast Cancer Research, 2019, 21, 61.	2.2	42
14	Impact of Freezing Delay Time on Tissue Samples for Metabolomic Studies. Frontiers in Oncology, 2016, 6, 17.	1.3	40
15	Lowâ€molecular contrast agent dynamic contrastâ€enhanced (DCE)â€MRI and diffusionâ€weighted (DW)â€MRI early assessment of bevacizumab treatment in breast cancer xenografts. Journal of Magnetic Resonance Imaging, 2013, 38, 1043-1053.	in 1.9	34
16	APIM-peptide targeting PCNA improves the efficacy of docetaxel treatment in the TRAMP mouse model of prostate cancer. Oncotarget, 2018, 9, 11752-11766.	0.8	33
17	Autocrine activin A signalling in ovarian cancer cells regulates secretion of interleukin 6, autophagy, and cachexia. Journal of Cachexia, Sarcopenia and Muscle, 2020, 11, 195-207.	2.9	31
18	Anti-vascular effects of the cytosolic phospholipase A2 inhibitor AVX235 in a patient-derived basal-like breast cancer model. BMC Cancer, 2016, 16, 191.	1.1	30

#	Article	IF	CITATIONS
19	Intravascular Targets for Molecular Contrast-Enhanced Ultrasound Imaging. International Journal of Molecular Sciences, 2012, 13, 6679-6697.	1.8	29
20	NMRâ€based metabolomics of biofluids in cancer. NMR in Biomedicine, 2019, 32, e3927.	1.6	29
21	In vivo MRI and histopathological assessment of tumor microenvironment in luminalâ€like and basalâ€like breast cancer xenografts. Journal of Magnetic Resonance Imaging, 2012, 35, 1098-1107.	1.9	27
22	Combined <sup>18</sup> F-Fluciclovine PET/MRI Shows Potential for Detection and Characterization of High-Risk Prostate Cancer. Journal of Nuclear Medicine, 2018, 59, 762-768.	2.8	27
23	Glycerophosphocholine (GPC) is a poorly understood biomarker in breast cancer. Proceedings of the National Academy of Sciences of the United States of America, 2012, 109, E2506; author reply E2507.	3.3	26
24	Subtypeâ€specific response to bevacizumab is reflected in the metabolome and transcriptome of breast cancer xenografts. Molecular Oncology, 2013, 7, 130-142.	2.1	26
25	MRI reveals the in vivo cellular and vascular response to BEZ235 in ovarian cancer xenografts with different PI3-kinase pathway activity. British Journal of Cancer, 2015, 112, 504-513.	2.9	25
26	A PET/MRI study towards finding the optimal [18F]Fluciclovine PET protocol for detection and characterisation of primary prostate cancer. European Journal of Nuclear Medicine and Molecular Imaging, 2017, 44, 695-703.	3.3	25
27	O-GlcNAc Transferase Inhibition Differentially Affects Breast Cancer Subtypes. Scientific Reports, 2019, 9, 5670.	1.6	23
28	Inhibition of O-GlcNAc transferase activates tumor-suppressor gene expression in tamoxifen-resistant breast cancer cells. Scientific Reports, 2020, 10, 16992.	1.6	21
29	Phosphatase of regenerating liverâ€3 regulates cancer cell metabolism in multiple myeloma. FASEB Journal, 2021, 35, e21344.	0.2	19
30	<sup>13</sup> C Highâ€resolutionâ€magic angle spinning MRS reveals differences in glucose metabolism between two breast cancer xenograft models with different gene expression patterns. NMR in Biomedicine, 2011, 24, 1243-1252.	1.6	18
31	Quantitative <sup>31</sup> P HRâ€MAS MR spectroscopy for detection of response to PI3K/mTOR inhibition in breast cancer xenografts. Magnetic Resonance in Medicine, 2014, 71, 1973-1981.	1.9	18
32	Metabolic Response to Everolimus in Patient-Derived Triple-Negative Breast Cancer Xenografts. Journal of Proteome Research, 2017, 16, 1868-1879.	1.8	17
33	Diffusionâ€weighted MRI for early detection and characterization of prostate cancer in the transgenic adenocarcinoma of the mouse prostate model. Journal of Magnetic Resonance Imaging, 2016, 43, 1207-1217.	1.9	15
34	Detection and Differentiation of Breast Cancer Sub-Types using a cPLA2α Activatable Fluorophore. Scientific Reports, 2019, 9, 6122.	1.6	15
35	Pharmacokinetics of Perfluorobutane after Intra-Venous Bolus Injection of Sonazoid in Healthy Chinese Volunteers. Ultrasound in Medicine and Biology, 2017, 43, 1031-1039.	0.7	13
36	Cytosolic Phospholipase A2 Alpha Regulates TLR Signaling and Migration in Metastatic 4T1 Cells. International Journal of Molecular Sciences, 2019, 20, 4800.	1.8	13

#	Article	IF	CITATIONS
37	Antiâ€angiogenic therapy affects the relationship between tumor vascular structure and function: A correlation study between micro–computed tomography angiography and dynamic contrast enhanced MRI. Magnetic Resonance in Medicine, 2017, 78, 1513-1522.	1.9	12
38	Multiparametric characterization of response to antiâ€angiogenic therapy using USPIO contrastâ€enhanced MRI in combination with dynamic contrastâ€enhanced MRI. Journal of Magnetic Resonance Imaging, 2018, 47, 1589-1600.	1.9	11
39	Classification and biomarker identification of prostate tissue from TRAMP mice with hyperpolarized 13C-SIRA. Talanta, 2021, 235, 122812.	2.9	11
40	Metabolic effects of signal transduction inhibition in cancer assessed by magnetic resonance spectroscopy. Molecular Oncology, 2011, 5, 224-241.	2.1	10
41	In Vivo <sup>31</sup> P magnetic resonance spectroscopic imaging (MRSI) for metabolic profiling of human breast cancer xenografts. Journal of Magnetic Resonance Imaging, 2015, 41, 601-609.	1.9	10
42	NMR-Based Prostate Cancer Metabolomics. Methods in Molecular Biology, 2018, 1786, 237-257.	0.4	9
43	Detection of Recurrent Prostate Cancer With 18F-Fluciclovine PET/MRI. Frontiers in Oncology, 2020, 10, 582092.	1.3	9
44	Reproducible Lipid Alterations in Patient-Derived Breast Cancer Xenograft FFPE Tissue Identified with MALDI MSI for Pre-Clinical and Clinical Application. Metabolites, 2021, 11, 577.	1.3	9
45	Non-Invasive Prostate Cancer Characterization with Diffusion-Weighted MRI: Insight from In silico Studies of a Transgenic Mouse Model. Frontiers in Oncology, 2017, 7, 290.	1.3	7
46	Biodistribution of Poly(alkyl cyanoacrylate) Nanoparticles in Mice and Effect on Tumor Infiltration of Macrophages into a Patient-Derived Breast Cancer Xenograft. Nanomaterials, 2021, 11, 1140.	1.9	7
47	Wholeâ€body section fluorescence imaging – a novel method for tissue distribution studies of fluorescent substances. Contrast Media and Molecular Imaging, 2009, 4, 73-80.	0.4	6
48	Identification of Metastasis-Associated Metabolic Profiles of Tumors by 1H-HR-MAS-MRS. Neoplasia, 2015, 17, 767-775.	2.3	6
49	EMT-Derived Alterations in Glutamine Metabolism Sensitize Mesenchymal Breast Cells to mTOR Inhibition. Molecular Cancer Research, 2021, 19, 1546-1558.	1.5	6
50	Biomarker Discovery Using NMR-Based Metabolomics of Tissue. Methods in Molecular Biology, 2019, 2037, 243-262.	0.4	5
51	Polymerization as a Strategy to Improve Small Organic Matrices for Low-Molecular-Weight Compound Analytics with MALDI MS and MALDI MS Imaging. ACS Applied Polymer Materials, 2021, 3, 4234-4244.	2.0	4
52	R2* Relaxation Affects Pharmacokinetic Analysis of Dynamic Contrast-Enhanced MRI in Cancer and Underestimates Treatment Response at 7 T. Tomography, 2019, 5, 308-319.	0.8	4
53	Detection of phenotypeâ€specific therapeutic vulnerabilities in breast cells using a CRISPR lossâ€ofâ€function screen. Molecular Oncology, 2021, 15, 2026-2045.	2.1	3
54	Argininosuccinate lyase is a metabolic vulnerability in breast development and cancer. Npj Systems Biology and Applications, 2021, 7, 36.	1.4	3

#	Article	IF	CITATIONS
55	A targeted molecular probe for colorectal cancer imaging. , 2008, , .		2
56	Abstract 1131: O-GlcNAc transferase inhibition in breast cancer cells. , 2017, , .		1
57	MR-Derived Biomarkers for Cancer Characterization. , 2017, , 409-431.		0
58	Abstract 3737: Inhibition of O-GlcNAc transferase in tamoxifen resistant breast cancer cells. , 2016, , .		0
59	Abstract 4412: Metabolic reprogramming in EMT - targeting regulatory nodes in mesenchymal cells. , 2017, , .		Ο
60	Investigation of Tumor Metabolism by High-resolution Magic-angle Spinning (HR-MAS) Magnetic Resonance Spectroscopy (MRS). New Developments in NMR, 2018, , 151-167.	0.1	0